U.P.B. Sci. Bull., Series C, Vol. 80, Iss. 2, 2018 ISSN 2286-3540

INVERSION SIMULATION FOR METAL PIPE ELECTROMAGNETIC PARAMETERS BASED ON INDUCTION MEASUREMENT METHOD

Yinchuan WU[1], Jiatian ZHANG[2]

For correction of metal casing effect in induction logging technology, the casing parameters are obtained. A measure model which consists of one transmitter and two receivers is modeled in cased hole. A formulation of the inverse problem of determination of the electromagnetic parameters of metal tubes from the receiver voltage measured at single frequency is presented. The objective function is constructed based on the least square principle and a multi-parameter search algorithm using golden section search is designed. The results show that: When the true conductivity of metal casing changes from 2×10^6 S/m to 8×10^6 S/m, the true relative permeability of metal casing changes from 50 to 100 and the quality coefficient ε is set to 0.1%, the relative error $\Delta\sigma_2$ of the casing conductivity can be a minimum of 0.0288% and a maximum of 0.1700%, the relative error $\Delta\mu_{2r}$ of the casing relative permeability can be a minimum of 0.0144% and a maximum of 0.1861% ,and the number of the optimum search is 14 or 15.

Keywords: Induction Measurement, Metal Pipe, Parameters Inversion, Golden Section Method

1. Introduction

The value of open hole induction logs as the primary source for determining hydrocarbon saturation is well established for reservoir formation evaluation in the oil industry [1]. Casing is commonly used to avoid collapse of well in oil fields by inserting metallic pipes into the borehole. Most oil wells are cased with pipes except for exploratory and newly drilled wells [2]. Steel is the most commonly used material for the pipes. Since steel casing is more electrically conductive (10^6s/m is a typical conductivity) and magnetically conductive (the range of relative permeability is 40-110) than the formation around the borehole, electromagnetic (EM) signals from the surrounding formation undergo sizable attenuation as they are transmitted across the casing [3]-[4]. Standard EM logging devices operate at frequencies (10kHz-100kHz) too high for their signals to penetrate casings. Once a borehole is cased, the formation behind the casing is

[1] Key Laboratory of Photoelectric Logging and Detecting of Oil and Gas of Ministry of Education, Xi'an Shiyou University, Xi'an 710065, Shaanxi, China, E-mail: ycwu1997@sina.com
[2] Key Laboratory of Photoelectric Logging and Detecting of Oil and Gas of Ministry of Education, Xi'an Shiyou University, Xi'an 710065, Shaanxi, China

virtually inaccessible to standard induction logging methods. Fortunately, some studies indicate that EM signals through steel casing can be detected at low frequencies [5]-[6].

Induction surveys all share the same physical principles [7]. A transmitter, usually a multi-turn coil of wire, carries an alternating current of frequency. This creates a time varying magnetic field in the surrounding formation which in turn, by Faradays' law, induces an electromotive force (EMF). This EMF drives currents in the formation which are basically proportional to the formation conductivity. Finally, a receiver is positioned in the same hole as the transmitter. The receiver measures the magnetic field arising from the transmitter and the secondary or induced currents in the formation. In cased hole, however, not only the formation but also the casing causes the magnetic fields, and the magnetic field of the formation is much weaker than the magnetic field of the casing. It is necessary to remove the influence of metal pipe. Since any variations in the rock conductivity can be masked by even minute changes in the casing dimensions and material properties (conductivity and permeability), a spatial low-pass filtering and measurement of the casing properties have been proposed for the casing effect correction [8]-[9]. The result of analytical computation shows that the casing is uncoupled from the surrounding formation, meaning that the induced current flowing in the formation has no effect on the current distribution within the casing [10]. In case the casing parameters as radius, thickness, conductivity and permeability are detected, the magnetic field of the casing is computed and the influence of metal pipe is removed. Inductive measurement of the oil-well casing properties is discussed by a number of authors. The main principle of the inductive measurements of the casing's properties is based on a careful section of the coil separation and excitation frequency. For the measurement of the inner radius one should use transmitter and receiver coils (known as caliper coils) placed next to each other or a single-coil method based on the impedance measurement, and the excitation frequency is on the order of 10kHz. For measurement of the wall thickness one uses so-called remote-field technique, where the coil separation is 2 to 5 times larger than the casing inner diameter and excitation frequency is on order of 10Hz. The casing electromagnetic parameters (conductivity and permeability) are measured using a transmitter-receiver pair at some distance.

In this paper, a measure model which consists of one transmitter and two receivers is modeled in cased hole. A formulation of the inverse problem of determination of the electromagnetic parameters of metal tubes from the receiver voltage measured at single frequency is presented. The objective function is constructed based on the least square principle. A multi-parameter search algorithm using golden section search is designed.

2. Forward problem

2.1 Induction Measurement Model

The model is given in Fig. 1. Because of the axial symmetry of the problem domain, it is convenient to employ the cylindrical coordinate system(r, φ, z). A transmitter coil *T* with radius a is positioned at $z = 0$, and two receiver coils R_1 and R_2 with same radius *a* are positioned at z_1 and z_2. The metal casing has inner radius *b* and wall thickness *d-b*. The casing material is assumed to be homogenous with electrical conductivity σ_2 and magnetic permeability μ_2 ($\mu_2 = \mu_{2r}\mu_0$, μ_{2r} and μ_0 are relative magnetic permeability and vacuum magnetic permeability respectively). The homogenous formation surrounding the casing has electrical conductivity σ_3 and magnetic permeability $\mu_3(\mu_3 = \mu_{3r}\mu_0)$, and σ_1 and μ_1 ($\mu_1 = \mu_{1r}\mu_0$) are electrical conductivity and magnetic permeability of the borehole, respectively.

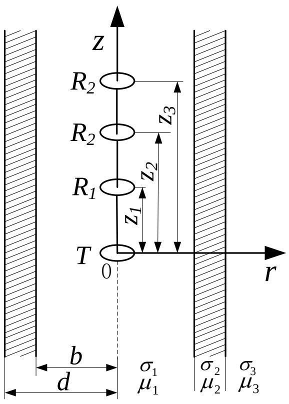

Fig. 1. Induction measurement model in metal casing

2.2 Electromagnetic in the borehole

In electric well logging, electromagnetic field change is analyzed through analytical method and finite element method. The analytical method has been used to successfully calculate electromagnetic field in axial symmetry model, while the finite element method is usually used in non-symmetry model. In this paper, a simplified axial symmetry model of induction measurement in metal casing is investigated, as shown in Fig. 1, therefore, the electromagnetic field is analyzed by the analytical method.

When the displacement current density is ignored, Maxwell's equations [11] are generally expressed in frequency domain as

$$\text{curl}\,\boldsymbol{H} = \sigma\boldsymbol{E} + \boldsymbol{J}_T \quad (1)$$

$$\text{curl}\,\boldsymbol{E} = -j\omega\mu\boldsymbol{H} \quad (2)$$

where $\boldsymbol{E}$ is the electric field, $\boldsymbol{H}$ the magnetic field, σ the conductivity, μ the magnetic permeability, ω the current angular frequency, $\boldsymbol{J}_T$ the source current distribution. Because of axial symmetry of the problem, the fields have specific directional components as

$$\boldsymbol{J_T} = \boldsymbol{J_T}(0, J_{T\varphi}, 0) \tag{3}$$

$$\boldsymbol{E} = \boldsymbol{E}(0, E_\varphi, 0) \tag{4}$$

and

$$\boldsymbol{H} = \boldsymbol{H}(H_r, 0, H_z) \tag{5}$$

Application of the curl operator in cylindrical coordinates in equations (1) and (2) gives

$$\frac{\partial H_r}{\partial z} - \frac{\partial H_z}{\partial r} = \sigma E_\varphi + J_{T\varphi} \tag{6}$$

$$\frac{\partial E_\varphi}{\partial z} = j\omega\mu H_r \tag{7}$$

and

$$\frac{1}{r}\frac{\partial (rE_\varphi)}{\partial r} = -j\omega\mu H_z \tag{8}$$

After elimination of H_z and H_r from equations (6), (7) and (8), E_φ satisfies

$$\frac{\partial^2 E_\varphi}{\partial r^2} + \frac{\partial^2 E_\varphi}{\partial z^2} + \frac{1}{r}\frac{\partial E_\varphi}{\partial r} + (k^2 - \frac{1}{r^2})E_\varphi = j\omega\mu J_{T\varphi} \tag{9}$$

where $k = \sqrt{-j\omega\mu\sigma}$, k is called the propagation constant in the medium. The homogenous form of equation (9) can be solved by separation variables. The solution has the form

$$E_\varphi(r,z) = -\frac{j\omega\mu M}{2\pi^2}\int_0^\infty [CI_1(\lambda r) + DK_1(\lambda r)]\cos(\xi z)d\xi \tag{10}$$

where $\lambda^2 = \xi^2 - k^2$ and $M = \pi a^2 N_T I_T$, M is the magnetic dipole moment of the transmitter coil, N_T the number of turns of the transmitter coil, $I_T = \int J_{T\varphi} ds$ the current of the transmitter coil, C and D undetermined coefficients, $I_1(\lambda r)$ and $K_1(\lambda r)$ the modified Bessel functions of the first and second kinds of order 1. Using the relation between H_r and E_φ in equation (6), $H_r(r,z)$ is expressed by

$$H_r(r,z) = \frac{M}{2\pi^2}\int_0^\infty \xi[CI_1(\lambda r) + DK_1(\lambda r)]\sin(\xi z)d\xi \tag{11}$$

Using the relation between H_z and E_φ in equation (7), $H_z(r,z)$ is expressed by

$$H_z(r,z) = \frac{M}{2\pi^2}\int_0^\infty \lambda[CI_0(\lambda r) - DK_0(\lambda r)]\cos(\xi z)d\xi \tag{12}$$

where $I_0(\lambda r)$ and $K_0(\lambda r)$ are the modified Bessel functions of the first and second kinds of order 0.

In the cased hole, the electromagnetic fields must satisfy the following conditions [12]:

(1)Near the transmitting coils, *E* and *H* are limited value.

(2)Far from the transmitting coils, *E* and *H* tend to zero.

(3)At the two interfaces between borehole and casing, and between casing and formation, the interface condition here reduces to the continuity of horizontal electric fields and the vertical magnetic fields, that is

$$E_{i\varphi} = E_{(i+1)\varphi} \tag{13}$$

$$H_{iz} = H_{(i+1)z} \tag{14}$$

where i is one medium number and i+1 is the other medium number of the same interface.

In borehole, since the condition (1) is satisfied, the coefficient D in equations (10), (11) and (12) equals zero. The electromagnetic fields in borehole are expressed by

$$E_{1\varphi}(r,z) = -\frac{j\omega\mu_1 M}{2\pi^2}\int_0^\infty [C_1 I_1(\lambda_1 r) + \lambda_1 K_1(\lambda_1 r)]\cos(\xi z)d\xi \tag{15}$$

$$H_{1r}(r,z) = \frac{M}{2\pi^2}\int_0^\infty \xi[C_1 I_1(\lambda_1 r) + \lambda_1 K_1(\lambda_1 r)]\sin(\xi z)d\xi \tag{16}$$

$$H_{1z}(r,z) = \frac{M}{2\pi^2}\int_0^\infty \lambda_1[C_1 I_0(\lambda_1 r) - \lambda_1 K_0(\lambda_1 r)]\cos(\xi z)d\xi \tag{17}$$

In medium II (casing), the equations are

$$E_{2\varphi}(r,z) = -\frac{j\omega\mu_2 M}{2\pi^2}\int_0^\infty [C_2 I_1(\lambda_2 r) + D_2 K_1(\lambda_2 r)]\cos(\xi z)d\xi \tag{18}$$

$$H_{2r}(r,z) = \frac{M}{2\pi^2}\int_0^\infty \xi[C_2 I_1(\lambda_2 r) + D_2 K_1(\lambda_2 r)]\sin(\xi z)d\xi \tag{19}$$

$$H_{2z}(r,z) = \frac{M}{2\pi^2}\int_0^\infty \lambda[C_2 I_0(\lambda_2 r) - D_2 K_0(\lambda_2 r)]\cos(\xi z)d\xi \tag{20}$$

In medium III, since the condition (2) is satisfied, the coefficient C in equations (15), (16) and (17) equals zero. The electromagnetic fields in formation satisfy

$$E_{3\varphi}(r,z) = -\frac{j\omega\mu_3 M}{2\pi^2}\int_0^\infty D_3 K_1(\lambda_3 r)\cos(\xi z)d\xi \tag{21}$$

$$H_{3r}(r,z) = \frac{M}{2\pi^2}\int_0^\infty \xi D_3 K_1(\lambda_3 r)\sin(\xi z)d\xi \tag{22}$$

$$H_{3z}(r,z) = -\frac{M}{2\pi^2}\int_0^\infty \lambda_3 D_3 K_0(\lambda_3 r)\cos(\xi z)d\xi \tag{23}$$

At the two interfaces, the condition (3) is satisfied. Appling the boundary conditions yield the system equations, which can be obtained using matrix algebra

$$\begin{bmatrix} \mu_1 I_1(\lambda_1 b) & -\mu_2 I_1(\lambda_2 b) & -\mu_2 K_1(\lambda_2 b) & 0 \\ \lambda_1 I_0(\lambda_1 b) & -\lambda_2 I_0(\lambda_2 b) & \lambda_2 K_0(\lambda_2 b) & 0 \\ 0 & \mu_2 I_1(\lambda_2 d) & \mu_2 K_1(\lambda_2 d) & -\mu_3 K_1(\lambda_3 d) \\ 0 & \lambda_2 I_0(\lambda_2 d) & -\lambda_2 K_0(\lambda_2 d) & \lambda_3 K_0(\lambda_3 d) \end{bmatrix} \times \begin{bmatrix} C_1 \\ C_2 \\ D_1 \\ D_2 \end{bmatrix} = \begin{bmatrix} -\mu_1 \lambda_1 K_1(\lambda_1 b) \\ \lambda_1^2 K_0(\lambda_1 b) \\ 0 \\ 0 \end{bmatrix} \tag{24}$$

Solving the matrix equation (24)

$$C_1 = \frac{\lambda_1(A_1B_1 + A_2B_2)}{A_1B_3 - A_2A_3} \tag{25}$$

where

$$\begin{cases} A_1 = \mu_2\lambda_3 K_0(\lambda_3 d)K_1(\lambda_2 d) - \mu_3\lambda_2 K_0(\lambda_2 d)K_1(\lambda_3 d) \\ A_2 = \mu_2\lambda_3 I_1(\lambda_2 d)K_0(\lambda_3 d) + \mu_3\lambda_2 I_0(\lambda_2 d)K_1(\lambda_3 d) \\ A_3 = \mu_1\lambda_2 I_1(\lambda_1 b)K_0(\lambda_2 b) + \mu_2\lambda_1 I_0(\lambda_1 b)K_1(\lambda_2 b) \\ B_1 = \mu_1\lambda_2 K_1(\lambda_1 b)I_0(\lambda_2 b) + \mu_2\lambda_1 K_0(\lambda_1 b)I_1(\lambda_2 b) \\ B_2 = \mu_1\lambda_2 K_0(\lambda_2 b)K_1(\lambda_1 b) - \mu_2\lambda_1 K_0(\lambda_1 b)K_1(\lambda_2 b) \\ B_3 = \mu_2\lambda_1 I_0(\lambda_1 b)I_1(\lambda_2 b) - \mu_1\lambda_2 I_0(\lambda_2 b)I_1(\lambda_1 b) \end{cases} \tag{26}$$

Therefore, the expressions for the electromagnetic fields in borehole are obtained. Taking into account the axial symmetry, the electromotive voltage of the receiver can be expressed by

$$V(a,z,\sigma_2,\mu_2) = \oint E \cdot dl = \oint E_{1\varphi}(a,z,\sigma_2,\mu_2)dl = 2\pi a N_R E_{1\varphi} \tag{27}$$

where N_R is the number of turns of the receiver coil, σ_2 and μ_2 are inversion parameters of metal pipe, *z* is the receiver location, and *a* is the radius of coil. We can use equation (27) to predict an electromotive force of the receiver from given parameters (a, z, σ_2, μ_2). Such a problem is called the forward problem.

3. Inverse Problems

3.1 Theoretical Background

Experiments suggest physical theories, and physical theories predict the outcome of experiments. The comparison of the predicted outcome and observed outcome allows us to ameliorate the theory. If in the physical theory we include the physical parameters describing the system under study, then inverse problem theory is about the quantitative rules to be used for this comparison between predictions and observations. The inverse problem consists in using observed data to infer the model parameters. This paper sets the inverse problems that we want to solve in order to estimate the electromagnetic parameters in metal pipe. The mathematical expression [12] is written as

$$d_n = F_n(p_1, p_2, p_3 \cdots p_M, s_n) \tag{28}$$

where d_n stand for the set of the observable data and d_n belong to the data space, F_n stands for the forward model, $p_1, p_2, p_3 \cdots p_M$ stand for inverse parameters, and s_n stand for other parameters in forward model. (28) is a set of nonlinear equations, and the initial value of inverse parameters are

$P_0^T = (p_{10}, p_{20}, p_{30}, \cdots p_{M0})$

Appling Taylor series expansion, equation (28) is written as

$$d_n = y_n(P_0) + \sum_{i=1}^{M} \left(\frac{\partial F_n}{\partial p_i}\right)\Big|_{p_{io}} \delta p_i \tag{29}$$

Which can be obtained using matrix algebra

$$\varepsilon = d - y = J\Delta P \tag{30}$$

where

$$d = [d_1, d_2, d_3, \cdots d_N]^T$$
$$y = [y_1, y_2, y_3, \cdots y_N]^T$$
$$\varepsilon = [d_1 - y_1, d_2 - y_2, d_3 - y_3, \cdots d_N - y_N]^T$$
$$\Delta P = [p_1, p_2, p_3, \cdots p_M]^T$$
$$J = \begin{vmatrix} \frac{\partial F_1}{\partial p_1} & \cdots & \frac{\partial F_1}{\partial p_M} \\ \cdots & \cdots & \cdots \\ \frac{\partial F_n}{\partial p_1} & \cdots & \frac{\partial F_n}{\partial p_M} \end{vmatrix}$$

The objective function based on least-square criterion can be written as

$$\varphi(P) = \sum_{n=1}^{N} (d_n - y_n)^2 \tag{31}$$

The optimal parameters will be obtained when the objective function was minimized with some search algorithms. These algorithms are being applied progressively to the engineering. Optimal searching algorithms can be separated into two categories: requiring calculation derivative of the objective function and without requiring calculation derivative of the objective function [13]. The algorithms of requiring calculation derivative have the advantages of fast convergence speed and small number of convergence, while the algorithms of without requiring calculation derivative (direct optimization methods) have the advantages of simple programming and easy implementation. The direct optimization methods are applied to a few parameters inversion.

3.2 Inverse method

In this paper, inverse parameters are conductivity σ_{2inv} and permeability μ_{2inv} of metal tube. The inverse parameters are calculated as follows:

Step1: The measurement voltage is detected at two receivers R_1 and R_2 by simulation method.

Step2: The initial parameters (conductivity, permeability) and inverse parameters scope are set.

Step3: The inductive voltages are computed through forward equation (27).

Step4: If the computing voltage can match the measurement voltage, that is to say, the value of objective function is minimum, the inverse process completes and the optimal estimation of the parameters σ_{2inv} and μ_{2inv} are obtained. Otherwise, the parameters are adjusted by some search algorithms, these parameters are considered to be the new initial parameters, and the inductive voltages are recalculated in Step3 until the results meet the requirements [14].

3.3 Multi-parameters Golden Section Method

Golden section method [15]-[16] is usually one-dimension search algorithm for finding a local minimum of the function. The golden section method has many advantages such as simple programming and easy to computer implementation, and it has been widely applied in many engineering fields. In this paper the golden section method is extended to multidimensional case. A complex multidimensional section can be decomposed into a series of one-dimension questions to reduce the difficult of preparation.

The objective function is expressed as $f(x)$, and $x=(x_1,x_2,\cdots,x_n)^T$. Firstly, x_i $(i\neq 1)$ is fixed, the optimal x_1^1 in the interval (k_1^1,k_1^2) is searched by means of golden section method, and when $x_1=x_1^1$, a minimum $f(x)$ is achieved. Secondly, x_i $(i\neq 2)$ is fixed, the optimal x_2^1 in the interval (k_2^1,k_2^2) is searched by means of golden section method. And then, If this continues, x_3^1, x_4^1, $\cdots$,x_n^1 are obtained, and the first set of optimal parameters x^1 is found in n-dimensional space. On the basis of x^1, x^2 can be obtained in more narrow interval. The *j*th set of optimal parameters x^j can be described as follows:

$$x^j=(x_1^j,x_2^j,\cdots,x_n^j)^T \tag{32}$$

The same process is repeated until

$$\|x^m-x^{m-1}\|<\varepsilon\|x^m\| \tag{33}$$

and

$$|f(x^m)-f(x^{m-1})|<\varepsilon|f(x^m)| \tag{34}$$

where ε is algorithm quality coefficient, $\|\cdot\|$ is named a vector norms. Though the search direction of golden section method is not optimal, the method does not require derivatives. This algorithm has the advantages of fast convergence speed.

4. Numerical implementation and results

In Fig. 1, the borehole has an electrical conductivity $\sigma_1=0$ S/m and a magnetic permeability $\mu_1=\mu_0(\mu_0=4\pi\times 10^{-7}\,\mathrm{H/m})$. The inner casing radius *b* is 0.1m and the casing thickness *d-b* is 0.01m. The casing has an electrical conductivity $\sigma_2=(1-10)\times 10^6\ \mathrm{S/m}$ and a magnetic permeability $\mu_2=(40-100)\mu_0$. The formation has an electrical conductivity $\sigma_3=1\ \mathrm{S/m}$ and a magnetic permeability $\mu_1=\mu_0$. The transmitter coil *T* is a loop of wire of radius *a* = 0.03m and the number of turns $N_T=1000$, carrying 3A current at 100Hz. One receiver coil has fixed position z_1 =0.1m and the other has fixed position z_2=0.2m, and the number of turns $N_T=3000$.

4.1 Forward voltage characteristic

Fig. 2 shows that the real part and the imaginary of the receiver coil R_1 (z_1=0.1m) under different electromagnetic conditions. The real part of receiver voltage increases with growing of the conductivity and decreasing of permeability of the metal casing, while the imaginary part of receiver voltage decreases with growing of the conductivity and decreasing of permeability of the metal casing. It is shown that the real part and the imaginary of induced voltage are monotonic functions of the relative magnetic permeability and conductivity of the metal casing.

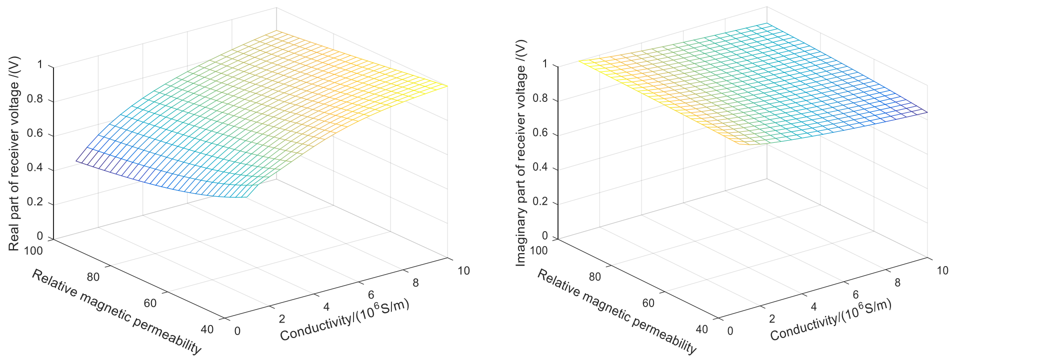

a) Real part of receiver voltage b) Imaginary part of receiver voltage

Fig. 2. Value of induced voltage as a function of relative magnetic permeability and conductivity (z_1 = 0.1m).

Fig. 3 shows that the real part and the imaginary of the receiver coil R_2 (z_2=0.2m) under different electromagnetic conditions. When the conductivity is greater than 2.5×10^6 S/m , the real part of receiver voltage increases with growing of the conductivity and decreasing of permeability of the metal casing. The maximum value of real part of receiver voltage occurs when the conductivity of metal casing is 1×10^6 S/m and relative magnetic permeability is 40. The imaginary part of receiver voltage decreases with growing of the conductivity and decreasing of permeability of the metal casing. It is shown that the imaginary of receiver voltage is a monotonic function of the relative magnetic permeability and conductivity of the metal casing.

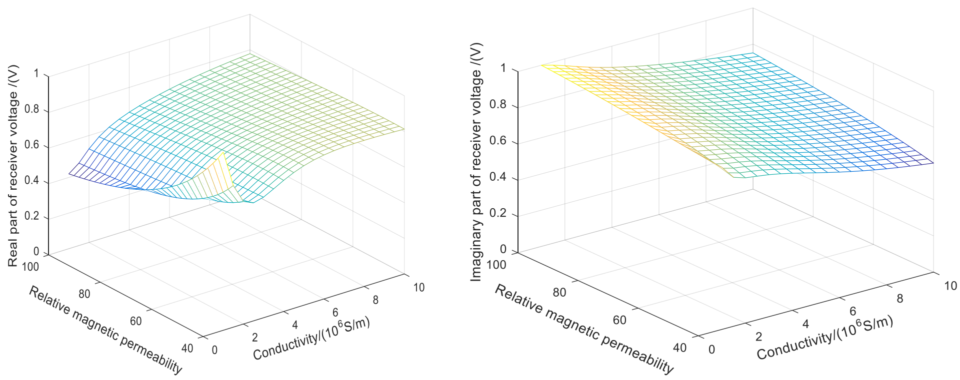

a) Real part of receiver voltage b) Imaginary part of receiver voltage

Fig. 3. Value of induced voltage as a function of relative magnetic permeability and conductivity (z_2= 0.2m).

4.2 Objective function characteristic

The objective function in this research is defined as equation (31). In equation (31), d_n is measuring voltage and y_n is calculating voltage. Specifically, N is equal to 4, d_1 is the real part of measuring voltage and y_1 is the real part of calculating voltage (z_1=0.1m), d_2 is the imaginary part of measuring voltage and y_2 is the imaginary part of calculating voltage (z_1=0.1m), d_3 is the real part of measuring voltage and y_3 is the real part of calculating voltage (z_2=0.2m), d_4 is the imaginary part of measuring voltage (z_2=0.2m) and d_4 is the imaginary part of calculating voltage (z_2=0.2m). The less in the voltage difference between measuring voltage d_n and calculating voltage y_n(the smaller the value of the objective function), the closer the inversion electromagnetic parameters are to that of true parameters. Once the minimum of objective function is obtained, the inversion results are acquired. The graph of the objective function is depicted in Fig. 4. Fig. 4 shows that the objective function has parabola-like shape, the Golden Section Search method can be used to search for the minimum value of a continuous objective function.

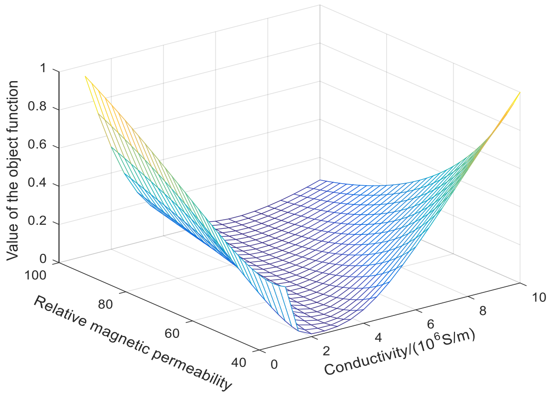

Fig. 4. Objective function as a function of relative magnetic permeability and conductivity.

4.3 Parameters inversion results

The results of parameters inversion are shown in Table1. K is the number of the optimum search(also called convergence speed), ε is quality control coefficient, σ_2 is the true conductivity of metal casing, $\mu_{2r}$is the true relative permeability of metal casing, σ_{2inv} is inversion conductivity and μ_{2rinv} is inversion relative permeability, The relative error $\Delta\sigma_2$ of the casing conductivity and the relative error $\Delta\mu_{2r}$ of the casing relative permeability are defined as

$$\Delta\sigma_2 = \frac{|\sigma_2 - \sigma_{2inv}|}{\sigma_2} \times 100\% \tag{35}$$

$$\Delta\mu_{2r} = \frac{|\mu_{2r} - \mu_{2rinv}|}{\mu_{2r}} \times 100\% \tag{36}$$

In table 1, the quality coefficient ε is set to 0.1%. When σ_2 is 2.0000×10^6 S/m and μ_{2r} is 50.0000, the inversion results show that the relative error $\Delta\sigma_2$ is

0.0551% , $\Delta\mu_{2r}$ is 0.0144% and the number K is 15; when σ_2 is 6.0000×10^6 S/m and μ_{2r} is 80.0000, the inversion results show that the relative error $\Delta\sigma_2$ is 0.1700% , $\Delta\mu_{2r}$ is 0.1816% and the number K is 14; when σ_2 is 8.0000×10^6 S/m and μ_{2r} is 100.0000, the inversion results show that the relative error $\Delta\sigma_2$ is 0.0288% , $\Delta\mu_{2r}$ is 0.0528% and the number K is 14.

As a result, the true conductivity σ_2 of metal casing changes from 2×10^6 S/m to 8×10^6 S/m, the true relative permeability μ_{2r} of metal casing changes from 50 to 100 and the quality coefficient ε is set to 0.1%. The true conductivity σ_2 and the true relative permeability μ_{2r} are simulation data. The inversion results show that $\Delta\sigma_2$ can be a minimum of 0.0288% and a maximum of 0.1700%, $\Delta\mu_{2r}$ can be a minimum of 0.0144% and a maximum of 0.1861%, the number of the optimum search is 14 or 15.

Table 1.

Parameters inversion results

The number K	coefficient ε	True value σ_2	μ_{2r}	Inversion results σ_{2inv}	μ_{2rinv}	Relative error $\Delta\sigma_2$	$\Delta\mu_{2r}$
15	0.1%	2.0000×10^6	50.0000	2.0011×10^6	49.9928	0.0551%	0.0144%
15	0.1%	4.0000×10^6	60.0000	4.0033×10^6	60.0575	0.0825%	0.0958%
14	0.1%	5.0000×10^6	70.0000	5.0051×10^6	70.0848	0.1020%	0.1211%
14	0.1%	6.0000×10^6	80.0000	6.0102×10^6	80.1489	0.1700%	0.1861%
14	0.1%	8.0000×10^6	100.0000	8.0023×10^6	99.9472	0.0288%	0.0528%

5. Conclusions

In a single cased hole, the casing is measured at single frequency by induction logging method and the electromagnetic parameters of metal casing are identified by multi-parameter inverse problem. The objective function is constructed based on the least square principle. A multi-parameter search algorithm using golden section search is designed. When the quality coefficient ε is set to 0.1%, the true conductivity of metal casing changes from 2×10^6 S/m to 8×10^6 S/m and the true relative permeability of metal casing changes from 50 to 100, the relative error $\Delta\sigma_2$ of the casing conductivity can be a minimum of 0.0288% and a maximum of 0.1700%, the relative error $\Delta\mu_{2r}$ of the casing relative permeability can be a minimum of 0.0144% and a maximum of 0.1861%.

Acknowledgments

This work was supported by Scientific Research Program of Shaanxi Provincial Education Department (Program No.16JK1605, No.15JS097).

REFERENCES

[1]. *Wu, J., Gong, H. S., Pang, J. F., Lu,T.* A New Signal Processing Method for the Dual Induction Measurement. Well Logging Technology, 27(1):11-15. 2003

[2]. *Wu, Y. C., Guo, B. L., Zhang, J. T.* Response Characteristics of Cased Hole Formation Resistivity Logging.International Journal of Earth Sciences and Engineering, 7(5):2075-2081. 2014

[3]. *Yang, W.* The Latest Progress and Developing Directions in Crosswell Electromagnetic Imaging. Well Logging Technology, 24(2):303-306. 2000

[4]. *Lu, H., Liu, J., Chen, L. R*. Influence of Wellbore Casing on Crosswell Electromagnetic Tomography Signal. Chinese Journal of Radio Science, 27(4):754-759. 2012

[5]. *Wei, B.J., Zhang, G.J., Ling, Q.J.* Influence of Metal Casing on Electromagnetic Logging Response. Geophysical Prospecting for Petroleum, 38(3): 67-75. 1999

[6]. *Hu, W. B., Xu, Z. P., Wang, J. M.* Study on Frequency Characteristics of Through Casing Electromagnetic responses, Journal of Oil and Gas Technology, 29(4):71-74. 2007

[7]. *Kaufman, A. A., Dashevsky, Y. A*. Principles of Induction Logging. Petroleum Industry Press: Beijing, 2013.

[8] *Hanshan Li, Sangsang Chen.* Detection Ability Mathematical Model and Performance Evaluation Method in Visible-Light Photoelectric Detection System. IEEE Sensors Journal, 17(6):1649-1655. 2017

[9]. *Vasic, D., Bilas, V.* Application of Stochastic Inversion to Casing Effect Correction in Through Casing Induction Logging, IEEE Transactions on Instrumentation and Measurement, 61(5): 1458-1465. 2012

[10]. *Wu, Y. C., Guo, B. L., Zhang, J. T.* Analysis and simulation of metal casing effect on induction logging, Optik,138:302-313. 2017

[11]. *Hayt, W. H., Buck, J. A.* Engineering electromagnetic, Tsinghua University Press: Beijing, 2009.

[12]. *Hanshan Li.* Space target optical characteristic calculation model and method in the photoelectric detection target. APPLIED OPTICS ,55(13):3689-3694. 2016

[13]. *Chen, B.L*. Optimization theory and algorithm, Tsinghua University Press: Beijing,2005.

[14]. *Wang, Y.F., I.E., V. N., A. G.* Inverse Problems in Geophysics and Solution Methods, Higher Education Press: Beijing, 2011.

[15]. *Tsai, C.H., Kolibal Joseph and Li, M. The* golden section search algorithm for finding a good shape parameter for meshless collocation methods. Engineering Analysis with Boundary Elements, 34:738-746. 2010

[16]. *Beltran-Royo, C.*, The Radar Method: An Effective Line Search for Piecewise Linear Concave Functions. Ann Oper Res, 166:299-312. 2009